Inquiro, the UAB undergraduate science research journal

Volume 2010 | Number 4 Article 28

2010

A screen designed to identify MKS-like genes yields a novel allele of mks-5

Rachel M. Stupay

Corey L. Williams

Svetlana V. Masyukova

Bradley K. Yoder

A Screen Designed to Identify MKS-like Genes Yields a Novel Allele of mks-5

Rachel M. Stupay, Corey L. Williams, Svetlana V. Masyukova, and Bradley K. Yoder
Department of Cell Biology, University of Alabama at Birmingham

Abstract

Cilia are developmentally essential organelles projecting from most mammalian cells. Altered cilia function underlies a group of autosomal recessive disorders including Nephronophthisis (NPHP) and Meckel-Gruber syndrome (MKS). Although several genetic loci are linked to these diseases, causative mutations have not been identified in the majority of patients. Conservation of NPHP and MKS genes in C. elegans *allows its utilization for studying these disorders. Previously, our research revealed that the NPHP and MKS proteins interact and function as two distinct complexes in a region at the base of the cilium called the transition zone (TZ). Single mutations in* nphp *or* mks *genes in* C. elegans *alone have minimal affects on ciliogenesis; however, a combination of mutations in* nphp *with a mutation in any* mks *gene alters cilia formation. This relationship was utilized in a forward EMS mutagenesis screen in* nphp *mutants to identify novel candidate* mks*-like genes. At least nine novel loci were identified. Here using non-complementation and sequencing analysis, one of the alleles* (yhw91) *was identified as a new* mks-5 *mutation within an exon-intron splice site. The* yhw91 *mutation disrupted the localization of MKS-3, another protein involved in the MKS complex at the TZ. Hierarchy analysis was subsequently performed to determine that anchoring of all other known MKS complex proteins was dependent on MKS-5 function. Correspondingly, MKS-5 protein was detected at the TZ, and its localization was unaltered by* mks *and* nphp *mutations. This insinuates that MKS-5 may be the core anchoring protein in the MKS portion of the TZ complex. Analysis of other genes identified in the EMS screen is ongoing. Ultimately, MKS families will be screened for mutations in the homologs of genes identified from this screen.*

Introduction

The autosomally recessive Nephronophthisis (NPHP)-associated disorders are heterogenic and affect a variety of organs. Also termed ciliopathies, these genetic disorders result from mutations affecting proteins of largely unknown function that localize to the cilium or to cilia subdomains. In the purest form of NPHP, cysts will develop within the corticomedullary border of the kidney. Symptoms are isolated to the kidneys with renal interstitial infiltration in addition to fibrosis, and basement membrane disruption along with tubular atrophy. More severe forms of NPHP-related ciliopathies such as Meckel-Gruber syndrome (MKS) involve mutations in additional organs. MKS patients typically do not live past birth or are naturally aborted earlier. The additional symptoms of this autosomal recessive lethal disorder are central nervous system malformations, occipital encephalocele, post-axial polydactyly, bowing limbs, severe heart malformations, and hepatic developmental defects. [4] There is extensive genetic overlap between MKS and NPHP with distinct mutations identified in shared genes. This indicates that disease severity (and thus, clinical diagnosis) is influenced by which gene is affected, the nature of the mutation in that gene, and the genetic background of the patient. Unfortunately, the causative lesion in most MKS and NPHP patients remains unidentified. Identifying the missing genes involved in these disorders is critical to ultimately understanding the cellular and molecular basis of the disease and in turn developing possible genetic therapeutic strategies. [10]

Homologs of at least ten NPHP and MKS genes have been identified in the nematode *C. elegans*, and thus far, their encoded proteins localize to the transition zone (TZ) at the base of sensory cilia. [9, 10, 11] Whereas humans have primary cilia extending from the majority of their cells, *C. elegans* only have sensory cilia extending from a subset of their neurons in the head (amphids) and tail (phasmids).

Cilia are microtubule-based and membrane-bound organelles. They develop via nucleation of microtubules templated by the centriole, which can remain attached to the proximal end of mature cilia as the basal body. The basal body helps anchor the cilium axoneme to the plasma membrane and cytoskeleton. The basal bodies function in the assembly of proteins that are involved in intraflagellar transport (IFT) in addition to initializing ciliogenesis. IFT is a critical component of cilia formation and it mediates the trafficking of proteins along the cilia axoneme. Just distal to the basal body is a ciliary subdomain called the TZ in which the cell membrane transitions to the cilium membrane. In the TZ region, Y-shaped links of unknown molecular composition protrude from the ciliary microtubules and form attachments with the surrounding membrane. Although the utility of the TZ is currently unclear, its positioning at the base of the cilium implicates a role as a regulator of protein movement between the cell and ciliary membrane. (Figure 1) When mutations occur within genes encoding the basal body, TZ, and IFT components in mice, symptoms of the aforementioned ciliopathies (diseases associated with ciliary defects) will result. In contrast to the critical requirement of cilia for mammalian development, the cilia of *C. elegans* function primarily as sensory organs and are not essential for the viability of the organism. The nonessential nature of the sensory cilia along with the genetic malleability of *C. elegans* facilitates the analysis of interactions between the large number of NPHP and MKS gene orthologues with relation to cilia structure and/or function. [6,10]

→ *top of page 58*

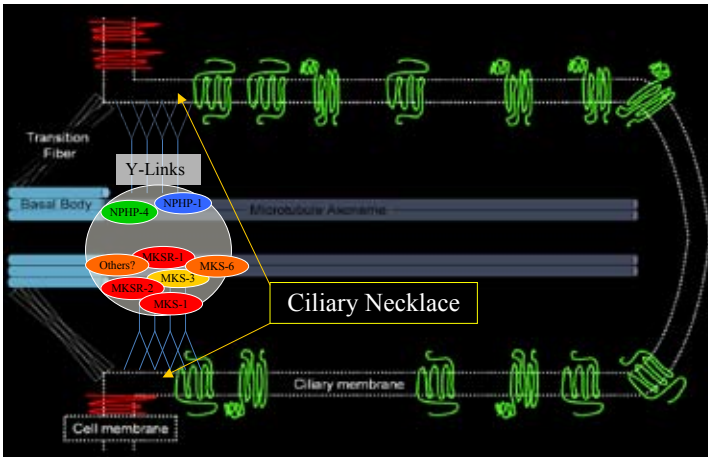

Figure 1. Anatomy of the cilium. The cilium features a membrane-encased microtubule backbone (axoneme) that protrudes from the cell surface. NPHP and MKS proteins are associated with the ciliary transition zone, which is a specialized region of the ciliary axoneme that connects to the basal body. The transition zone features Y-shaped links of unknown molecular composition that are attached to the transition zone microtubules and the surrounding ciliary membrane. This region of membrane is also known as the ciliary necklace as it features proteinacious decorations observable by electron microscopy. The transition zone is predicted to provide structural integrity to the cilium and to regulate protein trafficking into and out of the ciliary axoneme.

Genetic analyses have indicated the MKS and NPHP proteins form two distinct but potentially interacting functional complexes at the base of the cilia.[10, 11] Solitary mutations in genes in one complex will not cause a visible defect in cilia morphology in *C. elegans*; easily observable structural defects only arise when a combination of disruptions in both complexes is made. The disruption of cilia morphology in *mks;nphp* double mutant worms is most easily observed via a dye-filling assay in which the animals are exposed to a hydrophobic fluorescent dye. If cilia structure is normal, the dye is taken in through the cilia membrane and spreads throughout the sensory neurons. In the absence of properly formed cilia, the dye cannot stain the neurons; this phenomenon is referred to as a dye-filling defective (Dyf) phenotype. Any combination of mutations in the currently known *mks* genes with the *nphp-4(tm925)* mutation results in the Dyf phenotype (Figure 2).[9, 10, 11] Based on this phenomenon, we hypothesized that novel candidate MKS-like genes could be targeted in a mutagenesis screen for Dyf isolates in the context of the *nphp-4(tm925)* mutation. Once the mutants are identified from the *C. elegans* screen, an orthologue in the human genome might then be identified and screened in ciliopathy patients in whom a causative mutation has not been found. [10, 11]

Previously, an EMS (ethyl methane sulfate) mutagenesis screen was performed on *nphp-4(tm925)* mutant worms and ~200 Dyf F2 progeny were isolated (Svetlana Masyukova unpublished and[9]). A method of outcrossing with N2 Bristol males (wild-type) followed by subsequent phenotypic homozygous segregation analysis was utilized to filter new mutations as those independently causing the Dyf phenotype (1:3 Dyf versus wild-type segregation ratio) or those dependent on the presence of the *nphp-4(tm925)* allele for the Dyf phenotype (1:15 Dyf versus wild-type segregation ratio). (Figure 3) Through this outcrossing method, we uncovered ~40 new alleles (out of the original 200) that required the presence of the *nphp-4(tm925)* mutation to disrupt dye-filling.

Here, bulk segregate SNP analysis of the primary strain utilized in this study (YH972) showed linkage with chromosomes II (*novel mutation*) along with expected linkage with chromosome V at the *nphp-4* locus (Svetlana Masyukova unpublished).

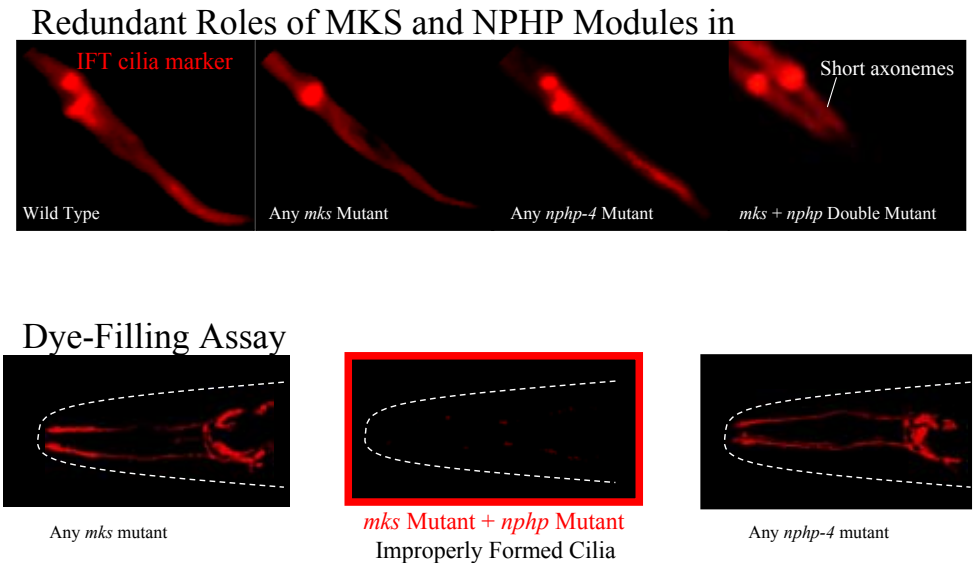

Figure 2. Redundant roles of MKS and NPHP modules in ciliogenesis

Figure 2a. Fluorescence images of worms expressing the cilia-specific IFT marker protein XBX-1::tdTomato in tail cilia pairs. Tail axoneme structure in mks and nphp single mutant worms is normal compared to wild type. In contrast, mks;nphp *double mutant worms have shortened cilia.*

Figure 2b. Fluorescence images of worms following exposure to DiI. mks *mutant worms and* nphp *mutant worms individually dye-fill normally, shown by the presence of DiI throughout the ciliated sensory neurons in the head. Combination of an* mks *mutation along with an* nphp *mutation in the same worm resulted in a failure to uptake dye due to alteration of cilia structure (see 2a).*

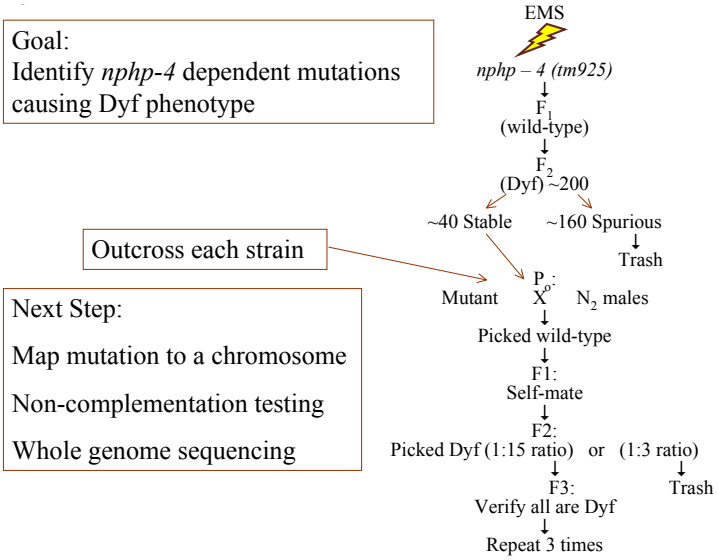

Figure 3. Outline of the mutagenesis screen performed on nphp-4 (tm925) *mutant worms.*

Non-complementation analysis was utilized to indicate that the YH972 mutation (*yhw91*) is a novel allele of the C09G5.8 gene, which is orthologous to human MKS-associated gene, *RPGRIP1L/MKS5*. [3] A base-pair mutation in the YH972 *mks-5*/C09G5.8 gene was detected by sequence analysis. Both the *yhw91* point mutation and an already characterized *mks-5(tm3100)* deletion mutation were utilized in mating schemes to visualize the phenotypic effect of the new point mutation obtained from the screen. Both *mks-5(yhw91)* and *mks-5(tm3100)* mutant animals were found to abrogate protein trafficking across the TZ . Additionally, the *yhw91* and *tm3100* mutations were both found to disrupt the localization of other MKS proteins at the TZ, which insinuates that the MKS-5 protein is required for normal localization of known MKS complex proteins. Interestingly, the localization of MKS-5 protein is unaltered by the loss of other MKS or NPHP proteins.

Procedure / Results

In previous studies chromosomal location was determined by bulk segregate analysis for each novel *nphp-4* dependent mutation generated in our EMS mutagenesis screen (Svetlana Masyukova unpublished, and summarized in Figure 4 and 5) [9]. As an attempt to validate whether the screen accurately targeted MKS-like genes we next determined whether any of these new mutations were in genes homologous to those already known to be associated with MKS in humans. This was accomplished by performing genetic non-complementation analysis between our newly mapped mutants and *mks-x;nphp-4* strains in which the corresponding *mks* gene was located on the same chromosome as the newly mapped mutation. Complementation is the term used to describe the phenomenon in which the mating between two animals with identical mutant phenotypes but with homozygous mutations in different genes produces offspring lacking the shared phenotype. This occurs because each parent will provide for its offspring one wild-type copy of the gene mutated in its mate. Alternatively, if both parents were homozygous mutant at the same locus, then their offspring would, as a rule, also be homozygous mutant and no phenotypic rescue would occur. This is referred to as non-complementation. This report focused on novel mutants that mapped to chromosome II. These include *yhw35, yhw36, yhw39, yhw91, yhw128,* and *yhw129*. Each strain was complementation tested against one another and against *mks-3* and *mks-5*, which both reside on chromosome II.

Allele	Linkage Group	Complementation Group
yhw35	Chr II	36, 39, 128, 129
yhw36	Chr II	35, 39, 128, 129
yhw128	Chr II	35, 36, 39, 129
yhw129	Chr II	35, 36, 39, 128
yhw91	**Chr II**	??????????
yhw65	Chr IV	66
yhw66	Chr IV	65
yhw3	Chr V	9, 15, 17, 19, 130, 131, 135
yhw9	Chr V	3, 5, 15, 17, 19, 130, 131, 135
yhw15	Chr V	3, 5, 9, 17, 19, 130, 131, 135
yhw17	Chr V	3, 5, 9, 15, 19, 130, 131, 135
yhw19	Chr V	3, 5, 9, 15, 17, 130, 131, 135
yhw130	Chr V	3, 5, 9, 15, 17, 19, 130, 135
yhw131	Chr V	3, 5, 9, 15, 17, 19, 130, 135
yhw135	Chr V	3, 5, 9, 15, 17, 19, 130, 131
yhw12	Chr V	68
yhw68	Chr V	12
yhw24	Chr X	26,71
yhw26	Chr X	24, 71
yhw71	Chr X	24,26

Figure 4. Novel nphp-4 *dependent mutations generated in the mutagenesis screen. Alleles are organized by linkage and complementation groups.*

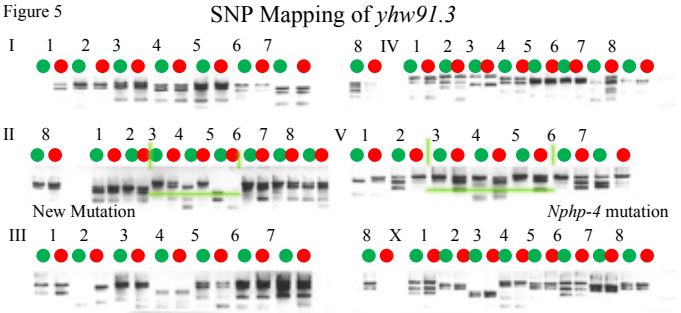

C. elegans gene	Chromosome number
nphp-1	II
nphp-4	V
mks-1	III
mksr-1	X
mksr-2	IV
mks-3	II
mks-5	II
mks-6	I

Figure 5. SNP mapping of yhw91 *indicates its location on chromosome II.*

Figure 5a. DraI *digest profile of SNP regions amplified from F2 progeny of* yhw91;nphp-4 *crossed with a SNP mapping strain. The first column of each SNP shows Dyf F2 progeny digest profile, and the second column shows wild type F2 sibbling digest profile.*

Figure 5b. Genomic location of the MKS and NPHP module genes in C. elegans. yhw91 *is found on the same chromosome as* mks-3 *and* mks-5.

The non-complementation testing of novel chromosome II mutants went as follows: *mks-3;nphp-4* or *mks-5;nphp-4* double mutant hermaphrodites were crossed to *nphp-4* males to produce *mks-3*$^{-/+}$*;nphp-4*$^{-/-}$ or *mks-5*$^{-/+}$*;nphp-4*$^{-/-}$ males that are capable of mating (cilia morphology mutants are not adequate maters due to the involvement male sensory ray cilia in mating activities). These males were then crossed with each novel chromosome II mutant (Figure 6). A similar strategy was used to cross each novel chromosome II mutant with one another. The readout for this assay was the presence or absence of Dyf male progeny. If no Dyf males arise (complementation), it is indicative that the parent strains have mutations in separate genes. If some Dyf males arise (non-complementation), then the parents have mutations in the same gene. Remarkably, our analysis showed non-complementation between *yhw35, yhw36, yhw39, yhw128,* and *yhw129*, indicating the mutations in these strains all affect the same gene on chromosome II (Figure 6). All of these mutants were able to complement *mks-3(tm2547)*, *mks-5(tm3100)*, and *yhw91*. *yhw91*, on the other hand, complemented *mks-3(tm2547)* but showed non-complementation with *mks-5(tm3100)* (Figure 6), indicating that the *yhw91* molecular lesion likely affected the *mks-5* gene. Morphology analysis using fluorescently-tagged cilia proteins revealed *yhw91;nphp-4* double mutants have abnormally formed cilia and fail to properly localize MKS-3 (Figure 7).

Figure 6

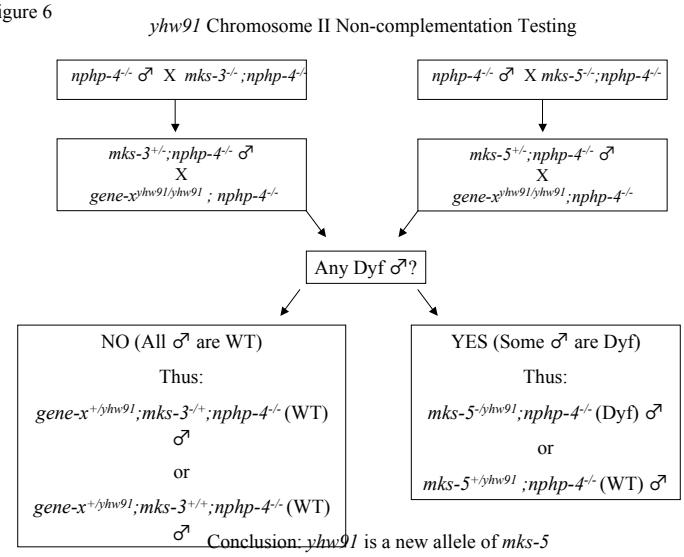

Figure 6. Non-complementation analysis of yhw91 *revealing its identity as a novel mks-5 allele.*

Figure 7

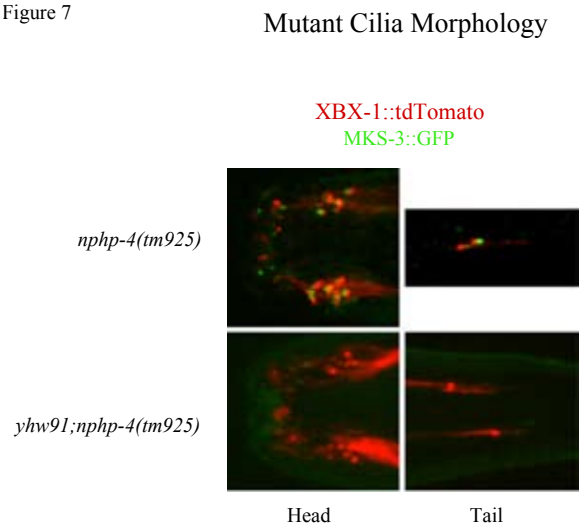

Figure 7. Fluorescence images of worms coexpressing XBX-1::tdtomato to mark cilia and MKS-3::GFP to mark transition zones. Compared to nphp-4(tm925) *single mutants,* yhw91;nphp-4 *double mutants have abnormally formed cilia and fail to properly localize MKS-3.*

We next wanted to sequence the *mks-5(yhw91)* genomic region to identify the location and nature of the mutation. First, a collection of primers were constructed in order to selectively sequence fragments of the roughly 12-kilobase gene. These primers were then used for PCR of genomic DNA isolated from *yhw91*, as well as N2 wild type controls. Through multiple primer sets, the entire genomic sequence of *mks-5* was obtained for *yhw91*, and we were able to identify a base-pair mutation exchanging a guanine for an adenine at the junction between exon and intron 20 (Figure 8). Through RT-PCR analysis of the mks-5 transcript in *yhw91* mutants, we confirmed this mutation was detrimental to splicing between exons 20 and 21 (Figure 9). The mutant transcript reads through the end of exon 20 into intron 20 and thereby introduces code for 17 new amino acids before reaching a stop codon (Figure 9). This indicates that the 84 C-terminal amino acids of MKS-5 will be absent in the *yhw91* mutant protein. Overall, our identification of a novel allele in a known *mks* gene indicates that the EMS screen was accurately designed to identify proteins that are potentially novel MKS proteins.

Apart from the observation that *mks-5;nphp-4* double mutants are synthetically Dyf, the function of MKS-5 in *C. elegans* has not been previously assessed. To examine the role of this protein, we utilized both the *yhw91* point mutation and the *tm3100* deletion mutation in assays for alterations in cilia function. For phenotypic analysis of the *yhw91* allele, we first outcrossed the *mks-5(yhw91);nphp-4(tm925)* double mutant with N2 worms to generate an F2 generation animal that was homozygous mutant at the *yhw91* locus and wild type at the *nphp-4* locus. This was accomplished by PCR and direct sequencing of the *yhw91*

locus in several F2 animals. Simultaneously, those animals were genotyped by PCR for the absence of the *nphp-4(tm925)* deletion mutation.

In a normal cell, some membrane-associated proteins are allowed to enter the ciliary axoneme, whereas others are kept out of the cilium. This barrier between the cilia and plasma membranes is hypothesized to the ciliary necklace, a portion of the membrane attached to TZ microtubules via Y-shaped links (Figure 1). In related studies, some *mks* mutations were found to disrupt cilia membrane composition by lack of regulation of protein trafficking across the TZ (Williams et al., in preparation). Specifically, upon disruption of MKS-associated and NPHP-associated genes, namely *nphp-1, nphp-4, mksr-1*, *mksr-2*, *mks-6*, and to a lesser extent *mks-1* and *mks-3*, restriction of the myristoylated membrane-associated protein RP2 from the ciliary membrane was markedly diminished. Thus, the TZ indeed appears to be responsible for keeping the protein content of the cilium membrane separate from the plasma membrane. Similar to what was observed in other *mks* mutants, the same defects were present in both *mks-5(yhw91)* and *mks-5(tm3100)* mutant animals (Figure 10), indicating that MKS-5 functions in a capacity similar to that of other MKS and NPHP proteins.

Figure 8

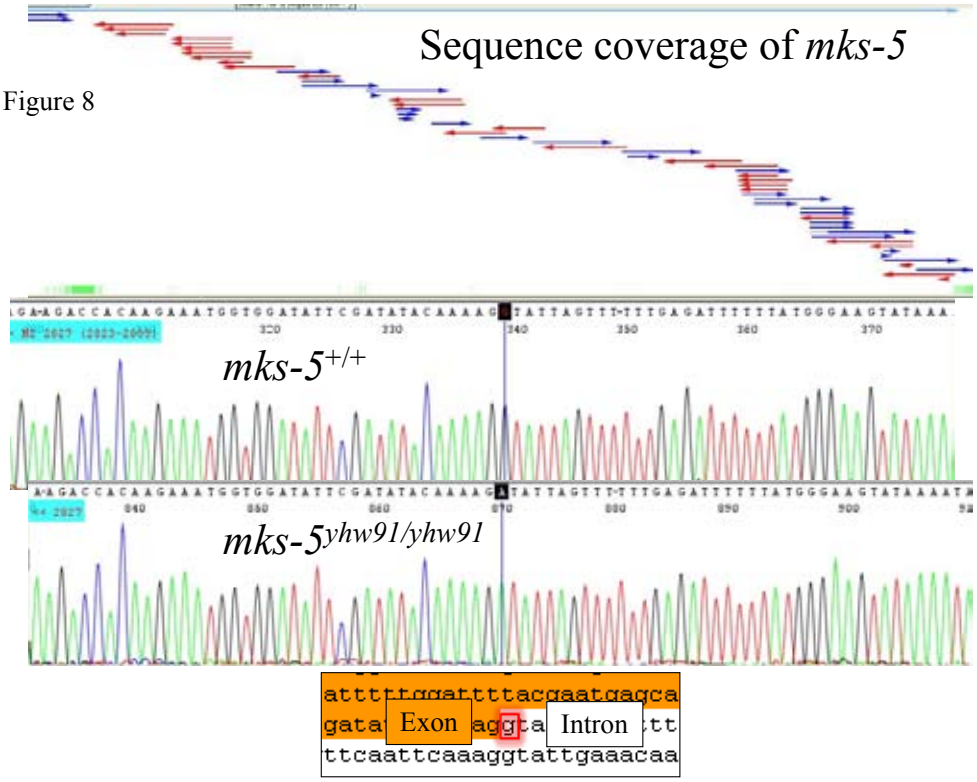

Figure 8. Sequence analysis of the mks-5(yhw91) *allele. Following whole gene sequencing analysis of* mks-5yhw91/yhw91 *mutant worms, a base pair mutation was identified at an intron-exon junction of exon 20.*

To further examine the potential role of MKS-5 and other MKS proteins in regulating ciliary membrane composition, we assessed the localization of the transmembrane-spanning TZ protein MKS-3. Normally, this protein is restricted at the TZ where it colocalizes with other MKS proteins. [10] However, in the background of either *mksr-1, mksr-2*, and our *mks-5* mutations, MKS-3 was no longer retained at the TZ and instead accumulated in the cilium membrane (Figures 10, 11, and 12) . This defect was not observed in either *nphp-1* or *nphp-4* mutants, which have altered RP2 levels in cilia, suggesting that the anchoring of MKS-3 at the TZ is MKS protein-specific (Williams *et al.*, in preparation).

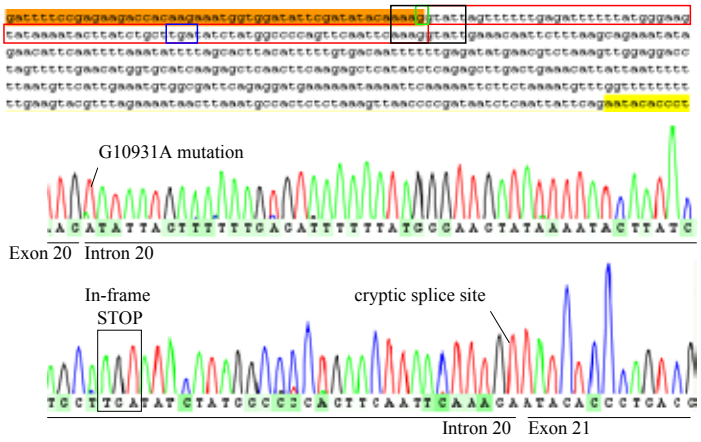

Figure 9. The yhw91 *mutation alters splicing of the* mks-5 *transcript. (Top) Sequence of* mks-5 *intron 20 region. A portion of exon 20 (orange), all of intron 20 (no coloration) and a portion of exon 21 (yellow) is shown. Nucleotide G10931 is boxed in green. (Bottom) Sequence trace of the* yhw91 *mutant transcript, showing readthrough at the mutated 10931 nucleotide into intron 20 (new sequence is highlighted in red above). Via a cryptic splice site in intron 21, splicing occurs with exon 21 downstream of an in-frame stop codon (blue box above). Interestingly, the cryptic splice site exactly matches the sequence at the end of exon 20 (black box).*

MKS-3/TMEM67 Ciliary Accumulation is *mks* Mutant-Specific. RP2 Accumulation also Occurs in *mks* Mutants.

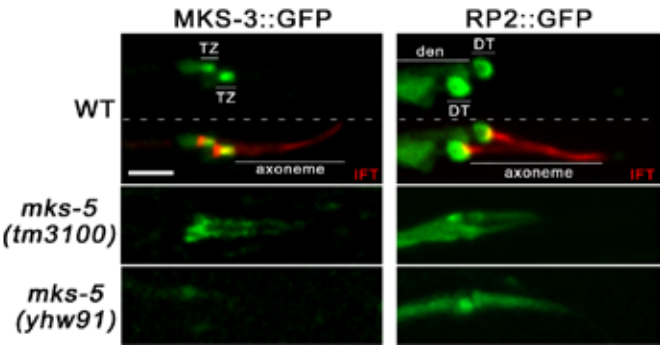

Figure 10. Cilia associated defects in mks-5(yhw91) *point mutants resemble those observed in* mks-5(tm3100) *deletion mutants. (left) Fluorescence images of worms expressing transmembrane MKS-3::GFP. Compared to wild type worms in which MKS-3 is enriched at the transition zone, MKS-3 was delocalized from the transition zone and accumulates in the ciliary axoneme when in the* mks-5(tm3100) *deletion mutant background. MKS-3::GFP was also delocalized from the transition zone in the* mks-5 (yhw91) *point mutant. This data shows that MKS-5 is essential for MKS-3 localization within the transition zone. (right) Similarly, the membrane-associated RP2::GFP protein also accumulated in cilia of both* mks-5(tm3100) *and* mks-5(yhw91) *mutants.*

Because MKS-3 TZ localization was lost in the background of *mks-5* mutations, we assessed whether other MKS proteins were dependent on MKS-5 for normal localization. A series of matings were set up to combine the *mks-5(tm3100)* mutation with each fluorophore-tagged MKS protein. These strains were then imaged along with control strains with the same transgenic markers in order to compare localization. Remarkably, *mks-5* was required for the localization of all other MKS proteins at the TZ (Figure 12). Since mammalian MKS5 (RPGRIP1L) was previously found to directly interact with NPHP4 [7], we also assessed whether disruption of *mks-5* in the worm would affect NPHP-4 TZ localization. Interestingly, upon loss of *mks-5* function, NPHP-4 (and NPHP-1) localization compared to wild type was restricted to a smaller region of the TZ (Figure 12). We were also interested in determining whether MKS-5 protein localized at the TZ along with the other MKS and NPHP proteins. By expressing tdTomato-tagged MKS-5 driven by the ciliated sensory neuron specific promoter of the *osm-5* gene, we were able to visualize MKS-5 localizing at the TZ at the base of cilia (Figure 12). Remarkably, the localization of MKS-5 was unaltered by the loss of other MKS or NPHP proteins (Figure 12). This observation along with the requirement of MKS-5 for the localization of all other known MKS proteins, suggests that MKS-5 is a major anchoring protein in a complex comprised specifically of MKS proteins, and to a lesser extent in the NPHP-1/4 complex (Figure 13).

Future endeavors

Based on this data, we have validated that the screen performed to identify novel genes functioning in similar fashion to known MKS genes is accurate in its intended goal. Additionally, we have discovered that MKS-5 is an essential component involved in the anchoring of the MKS and NPHP protein complexes. Further studies will involve the identification of molecular lesions in the additional genes resulting from the mutagenesis screen. Following their identification, these genes will be assessed for function in cilia and/or the TZ and their relationship to other MKS proteins. Ultimately, these novel MKS-like genes will be sequenced for mutations in human patients with cilia-related disorders. [5,8]

MKS Mutations Disrupt Ciliary Membrane Composition

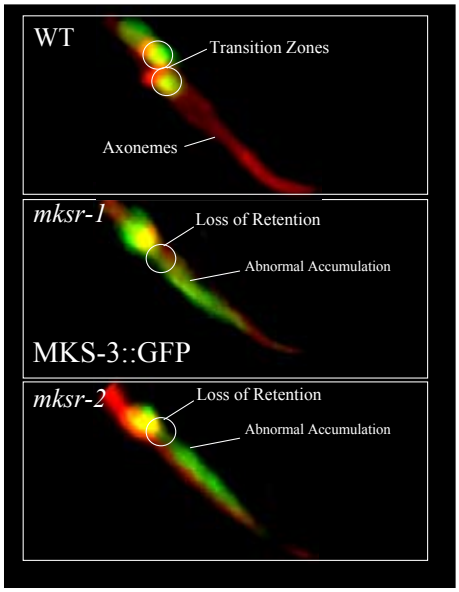

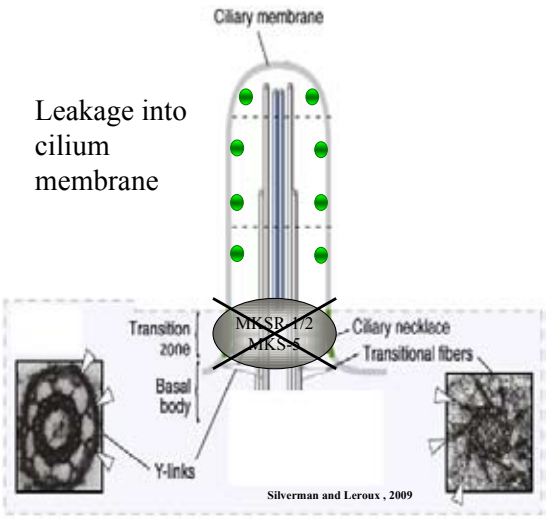

Figure 11. MKS-3 accumulates in the cilia of mksr-1 *and* mksr-2 *mutants. (left)Fluorescence images of worms coexpressing MKS-3::GFP and XBX-1::tdTomato (cilia marker). Similar to disruption of* mks-5 *(previous figure),* mksr-1 *and* mksr-2 *mutants also cause delocalization of* mks-3 *from the transition zone. (right) A model depicting accumulation of MKS-3 within the cilium membrane upon abrogation of MKSR-1, MKSR-2, or MKS-5 function.*

Figure 12

MKS-5 is essential for anchoring the MKS complex

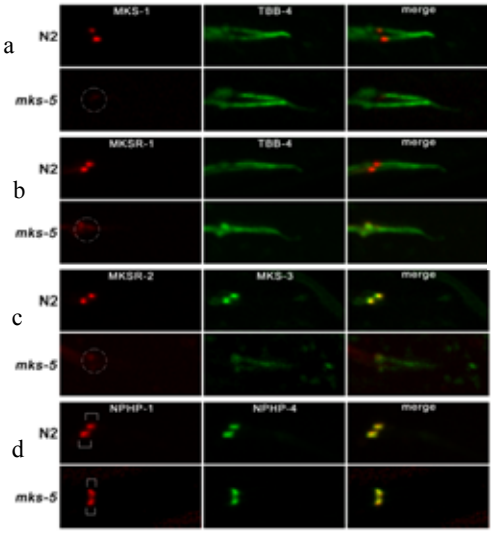

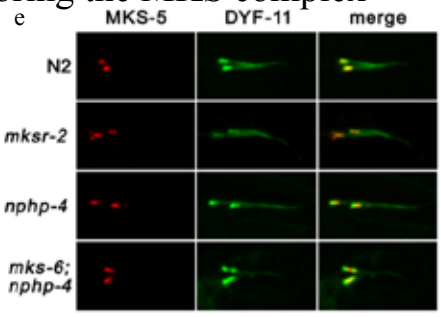

f

Gene	Required for Correct Localization of:
mks-1	None
mksr-1	MKS-1 [7], MKS-3, MKS-6 (Williams et. al, in submission)
mksr-2	MKS-1 [7], MKSR-1 [7], MKS-3, MKS-6 (Williams et. al, in submission)
mks-3	None
mks-5 (RPGRIP1L)	**Any MKS**: MKS-1, MKS-3, MKSR-1, MKSR-2, MKS-3, MKS-6 (Williams et. al, in submission)
mks-6	None
nphp-1	None
nphp-4	NPHP-1 [9]

Figure 12. MKS-5 is found at the transition zone where it is essential for anchoring the NPHP and MKS modules. a. Fluorescence images of worms coexpressing MKS-1::tdTomato and TBB-4(β-tubulin)::GFP. Compared to wild type (N2), MKS-1 is delocalized from the transition zone in mks-5(tm3100) *mutants. b. Fluorescence images of worms coexpressing MKSR-1::tdTomato and TBB-4(β-tubulin)::GFP. Compared to wild type (N2), MKSR-1 is delocalized from the transition zone in* mks-5(tm3100) *mutants. c. Fluorescence images of worms coexpressing MKSR-2::tdTomato and MKS-3::GFP. Compared to wild type (N2), both MKSR-2 and MKS-3 are delocalized from the transition zone in* mks-5(tm3100) *mutants. d. Fluorescence images of worms coexpressing NPHP-1::CFP and NPHP-4::YFP (psuedocolored red and green, respectively). Compared to wild type (N2), both NPHP-1 and NPHP-4 occupy a smaller region of the transition zone in* mks-5(tm3100) *mutants. e. Fluorescence images of worms coexpressing MKS-5::tdTomato and DYF-11::GFP. In wild type (N2) worms, MKS-5 localizes to the transition zone and is unaffected in* mksr-2 *and* nphp-4 *mutants, and a combination* mks-6/nphp-4 *mutant. f. Localization requirement results from the hierarchy screen.*

References

1. Bialas, N.J., Inglis, P.N., Li, C., Robinson, J.F., Parker, J.D., Healey, M.P., Davis, E.E., Inglis, C.D., Toivonen, T., Cottell, D.C., Blacque, O.E., Quarmby, L.M., Katsanis, N., Leroux, M.R. (2009). Functional Interactions Between the Ciliopathy-Associated Meckel Syndrome 1 (MKS1) Protein and Two Novel MKS1-Related (MKSR) Proteins. *J Cell Sci* **122**, 611-24.

2. Davis, M.W., Hammarlund, M., Harrach, T., Hullett, P., Olsen, S., Jorgensen, E.M. (2005). Rapid Single Nucleotide Polymorphism Mapping in *C. elegans*. BMC Genomics 6:1 18.

3. Delous, M., Baala, L., Salomon, R., Laclef, C., Vierkotten, J., Tory, K., Golzio, C., Lacoste, T., Besse, L., Ozilou, C., Moutkine, I., Hellman, N. E., Anselme, I., Silbermann, F., Vesque, C., Gerhardt, C., Rattenberry, E., Wolf, M. T. F., Gubler, M. C., Martinovic, J., Encha-Razavi, F., Boddaert, N., Gonzales, M., Macher, M. A., Nivet, H., Champion, G., Berthe´le´me´, J. B., Niaudet, P., McDonald, F., Hildebrandt, F., Johnson, C. A., Vekemans, M., Antignac, C., Ru¨ther, U., Schneider-Maunoury, S., Attie´-Bitach, T., & Saunier, S. The Ciliary gene RPGRIP1L is mutated in cerebello-oculo-renal syndrome (Joubert syndrome type B) and Meckel syndrome. Nature Genet. 39, 875-881.

4. Fliegauf, M., Horvath, J., von Schnakenburg, C., Olbrich, H., Muller, D., Thumfart, J., Schermer, B., Pazour, G. J., Neumann, H. P. H., Zentgraf, H., Benzing, T., Omran, H. (2006) Nephrocystin Specifically Localizes to the Transition Zone Renal and Respiratory Cilia and Photoreceptor Connecting Cilia. *J Am Soc Mephrol* 17: 2424-2433. doi: 10.1681/ASN.2005121351.

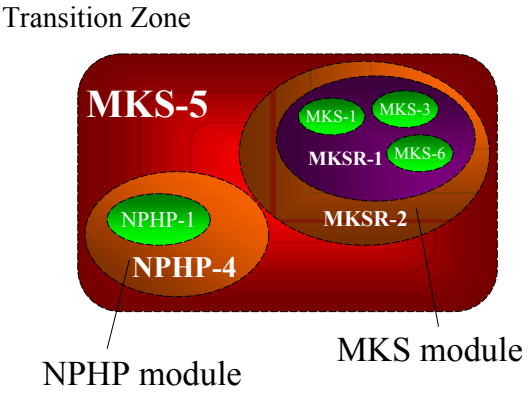

Figure 13. Hierarchical model for the ciliary transition zone functional modules. In the MKS module, MKS-1, MKS-3, and MKS-6 require MKSR-1 for transition zone localization, and MKSR-1 requires MKSR-2. MKS-5 is required for transition zone localization of each protein within the MKS module. In the NPHP module, NPHP-1 requires NPHP-4 for transition zone localization. NPHP-1 and NPHP-4 require MKS-5 for localization to a transition zone subdomain.

5. Hillier, L. W., Marth, G. T., Quinlan, A. R., Dooling, D., Fewell, G., Barnett, D., Fox, P., Glasscock, J. I., Hickenbotham, M., Huang, W., Margrini, V. J., Richt, R. J., Sander, S. N., Stewart, D. A., Stromberg, M., Tsung, E. F., Wylie, T., Schedl, T., Wilson, R. K., and Mardis, E. R. (2008). Whole-Genome Sequencing and Variant Discovery in *C. elegans*. Nature Methods 5:2 183-188.

6. Jorgensen, E. M., and Mango, S. E. (2002). The Art and Design of Genetic Screens: Caenorhabiditis elegans. Nature Publishing Group. www.nature.com/reviews/genetics. 3. 353-368.

7. Mollet, G., Salomon, R., Gribouval, O., Silbermann, F., Bacq, D., Landthaler, G., Milford, D., Nayir, A., Rizzoni, G., Antignac, C., Saunier, S. (2002) The gene mutated in juvenile nephronopthisis type 4 encodes a novel protein that interacts with nephrocystin. Nature Genet. 32, 300-305.

8. Shen, Y., Sarin, S., Liu, Y., Hobert, O., and Pe'er, I. (2008) Comparing Platforms for C. elegans Mutant Identification Using High-Throughput Whole-Genome Sequencing. PLoS ONE 12, e4012. 1-6.

9. Stupay, R. M., Williams, C. L., Masyukova, S., Yoder, B. K. (2010) A *Caenorhabiditis elegans* Mutagenesis Screen to Identify Candidate Human Cystic Kidney Disease Genes. Inquiro, Undergraduate Journal Vol. 3, 37-45.

10. Williams, C. L., Winkelbauer, M. E., Schafer, J. C., Michaud, E. J. and Yoder, B. K. (2008). Functional Redundancy of the B9 Proteins and Nephrocystins in Caenorhabiditis elegans Ciliogenesis. *Mol Biol Cell* **19**, 2154-2168.

11. Williams, C. L., Masyukova, S. V., Yoder, B. K. (2010). Normal Ciliogenesis Requires Synergy between the Cystic Kidney Disease Genes MKS-3 and NPHP-4. J Am Soc Nephrol.

12. Winkelbauer, M. E., Schafer, J. C., Haycraft, C. J., Swoboda, P. and Yoder, B. K. (2005). The *C. elegans* Homologs of Nephrocystin-1 and Nephrocystin-4 are Cilia Transition Zone Proteins Involved in Chemosensory Perception. *J Cell Sci* **118**, 5575-87.

13. Yook, K. (2005). Compelmentation. *WormBook,* ed. The *C. elegans* Research Community, WormBook, doi/10.1895/wormbook.1.24.1, http://www.wormbook.org.